Available online at www.sciencedirect.com
SCIENCE DIRECT®
Journal of Colloid and Interface Science 274 (2004) 103–106
JOURNAL OF Colloid and Interface Science
www.elsevier.com/locate/jcis

Nonspherical ZnS colloidal building blocks for three-dimensional photonic crystals

C.M. Liddell * and C.J. Summers

School of Materials Science and Engineering, Georgia Institute of Technology, Atlanta, GA 30332, USA

Received 8 August 2003; accepted 8 December 2003

Abstract

The asymmetry introduced by a complex or nonspherical basis promotes photonic band gap formation in three-dimensional photonic crystals. However, relatively few techniques have been demonstrated to produce uniform nonspherical colloids for use as photonic crystal bases. Here we expand the menu of basis types with high refractive index by preparing nonspherical zinc sulfide colloids of uniform size and shape. Dimers, trimers, and planar tetramers were precipitated from aqueous solution by the thermal decomposition of thioacetamide in the presence of zinc nitrate, manganese nitrate, and nitric acid. The well-defined morphological types were obtained from suspensions aged for 4–6 h at 26–32 °C and then for 20–35 min at 85 °C. Stereological techniques were used to analyze SEM images and determine the percentage of each particle class. For example, the quantitative characterization of a particle population prepared at 29 °C for 6 h and 85 °C for 22 min had the composition $59 \pm 3\%$ spheres, $31 \pm 2\%$ dimers, $7 \pm 1\%$ trimers, $0.4 \pm 0.2\%$ tetramers, and $2.5 \pm 0.8\%$ complex clusters (encompasses all other varieties of shape). X-ray diffraction and X-ray photoelectron spectroscopy confirmed the zinc blend crystal structure and the stoichiometric composition of the particles. The refractive index was estimated as 2.25 (413 nm)–2.09 (709 nm) by fitting experimental absorption spectra to curves derived from Mie scattering calculations. This indicated an average porosity ∼24%. Such colloids offer the potential to form diamond-like lattices with large, stable photonic band gaps.

Keywords: Zinc sulfide; Refractive index; Colloids; Photonic crystal; Nonspherical; Basis

1. Introduction

Several of the most promising applications of photonic crystals require the practical realization of a photonic band gap in the near-IR and visible regions [1–3]. The width and stability of the optical band gap in a photonic crystal strongly depend on the crystal structure and the refractive index contrast (n_c) between the basis of the structure and the surrounding matrix. Currently, many colloid-based photonic crystals have the inverse FCC sphere structure and are constructed by a self-assembly, infiltration, and etching process [4]. The inverse FCC structure exhibits a bandgap between the eighth and ninth photonic bands when the refractive index contrast is sufficient ($n_c > 2.9$). However, geometrical nonuniformity such as variation in the radii of spheres or random displacements from lattice sites reduces the band gap of inverse opals. Disorder as small as 2% of the lattice constant has been calculated to close the band gap regardless of high refractive index contrast.

Band gaps between lower lying bands, such as those that occur in the case of the diamond structure, are predicted to be much less sensitive to disorder [5]. Li et al. proposed the FCC arrangement of nonspherical dimer building blocks to mimic the diamond structure, which has two dielectric spheres per lattice point [6]. The diamond structure has the widest, most stable band gap [7], but is thermodynamically impossible to form by the traditional method of self-assembly of spheres. Self-assembly generally leads to structures with higher packing density such as simple FCC [8]. For the diamond-analog dimer lattice, both the asymmetry and the openness of the diamond structure are preserved. In fact, the filling fractions of high-index material are identical, 34%, for dimers aligned along the ⟨111⟩ crystallographic direction [6].

In this work, nonspherical particles were synthesized to provide high-refractive-index colloidal building blocks for complex lattices such as the diamond-analog structure.

* Corresponding author.
E-mail address: cliddel@ccmr.cornell.edu (C.M. Liddell).

0021-9797/$ – see front matter
doi:10.1016/j.jcis.2003.12.012

Chemical and optical characterization to evaluate the suitability of the colloids for photonic crystal applications was performed and is reported here.

2. Experimental

Colloidal suspensions of ZnS were prepared by the thermal decomposition of thioacetamide (TAA, CH_3CSNH_2) in acidic solutions of metal salt [9,10]—0.143 M TAA was added to mixed cation solutions of 0.024 M $Zn(NO_3)_2 \cdot 6H_2O$ and 0.00048 M $Mn(NO_3)_2 \cdot 4H_2O$ at room temperature. The solutions were acidified with 0.800 ± 0.001 ml of 15.8 M HNO_3 to ensure that the sulfide ions were released slowly enough to obtain monodisperse particles during precipitation. The reaction vessels were immersed in a thermostated water bath and aged for 4–6 h at 26–32 °C followed by a second constant-temperature treatment for 20–35 min at 85 °C. To end the reaction, suspensions were quenched in an ice bath to below 10 °C and the ZnS particles were separated from the mother liquid by several cycles of centrifugation and redispersion in water. The particles were collected by filtration on 0.22-μm cellulose ester membranes.

The particle morphology was examined in the LEO 1530 thermally-assisted field emission gun scanning electron microscope at 5 kV. X-ray diffraction spectra were obtained with a Philips PW 1800 automated powder diffractometer. ZnS particles were dusted onto clear tape and taped to the diffractometer solid sample mount. Particles were examined with monochromatized CuK_α radiation, $\alpha_1 = 1.54056$. X-ray photoelectron spectroscopy (XPS) was performed on an SSX-100 ESCA spectrometer manufactured by Surface Science Instruments. For the measurements, ZnS powder was contained in an aluminum foil boat and irradiated with monochromatized AlK_α X-rays at 1486.6 eV. Absorption/extinction spectra were recorded using a Beckman DU 640 transmission spectrophotometer over a wavelength scan range from 200 to 1100 nm. Gas adsorption measurements were performed using the Coulter SA 3100 surface area and pore size analyzer. Particles were placed in a 3-ml Coulter RapiTube sample tube and outgassed in nitrogen at 300 °C for 3 h prior to analysis to eliminate moisture from the pores. For the measurement of the gas adsorption and desorption isotherms, nitrogen was the adsorbate and helium was the carrier gas.

3. Results and discussion

Nonspherical particles having close-packed morphology types including dimers and trimers, as indicated in Fig. 1, were observed by scanning electron microscopy. Fig. 1a shows the ZnS particles precipitated by aging reactants for 5 h at 29 °C and 20 min at 85 °C. The particle morphology distribution was determined as $72.15 \pm 2.54\%$ spheres, $23.35 \pm 1.87\%$ dimers, $3.62 \pm 0.99\%$ trimers, $0.18 \pm 0.24\%$ tetramers, and $0.71 \pm 0.35\%$ complex clusters from 10 microstructural fields each containing more than 200 particles. The most uniform and monodisperse particles were obtained under these conditions. Fig. 1b shows particles prepared by aging reactants for 6 h at 29 °C and 22 min at 85 °C for comparison. In this case, the particle morphology distribution was $59 \pm 3\%$ spheres, $31 \pm 2\%$ dimers, $7 \pm 1\%$ trimers, $0.4 \pm 0.2\%$ tetramers, and $2.5 \pm 0.8\%$ complex clusters. A greater abundance of ZnS clusters were produced using these conditions; however, the level of control of the clustering was reduced, as indicated by the greater number of complex clusters.

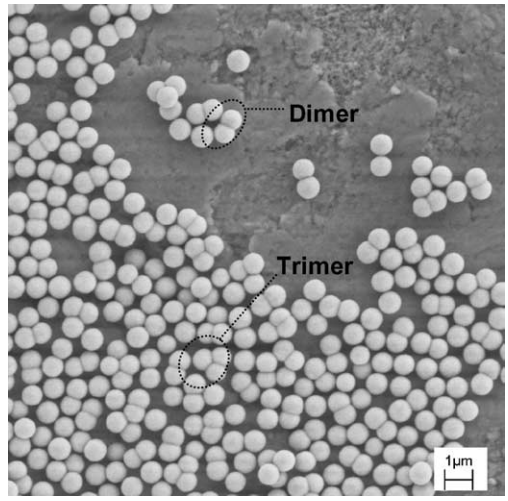

(a)

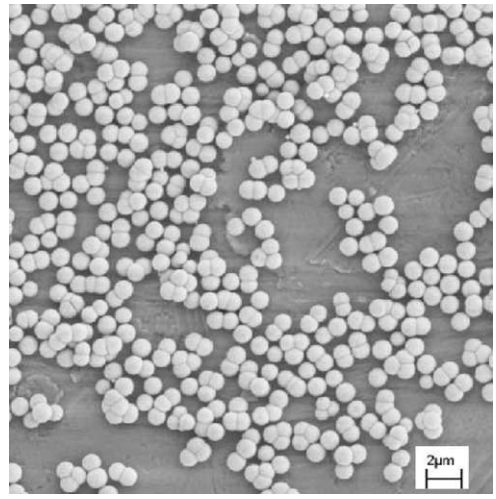

(b)

Fig. 1. SEM images of sample prepared by aging reactants for (a) 5 h at 29 °C and 20 min at 85 °C and (b) 6 h at 29 °C and 22 min at 85 °C.

3.1. Crystallinity and solid phase structure

The diffraction data confirmed the crystalline phase as zinc blend. X-ray diffraction peaks were indexed to the planes of sphalerite, cubic-phase ZnS structure (JCPDS Card 05-0566), as shown in Fig. 2a. Using X-ray line-

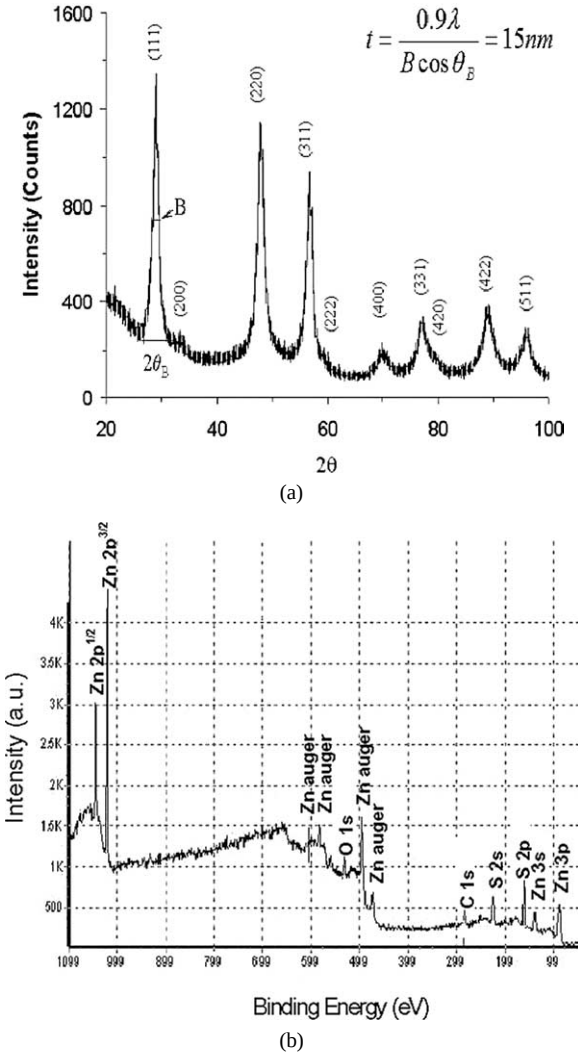

Fig. 2. (a) X-ray diffraction pattern and (b) XPS spectrum of ZnS particles.

broadening measurements on the three highest intensity peaks led to a primary crystallite size (t) estimate of 15 nm. Thus, the colloids are aggregates of nanocrystals.

The XPS spectrum provided in Fig. 2b shows binding energies of Zn2$p^{1/2,\,3/2}$, Zn3s, Zn3p, O1s, C1s, S2s, and S2p. Several Zn Auger electron peaks were also detected. Oxygen and carbon impurities may arise from water and unreacted TAA trapped within the particles.

The crystalline quality and phase structure purity suggest the capability of achieving the bulk value of the refractive index, 2.43 (488 nm), for the ZnS colloids. However, the formation of ZnS colloids by the aggregation of nanocrystals, as indicated by X-ray diffraction, does not occur in a volume-filling manner and in general leads to lower refractive index values [11,12].

3.2. Porosity and refractive index

The porosity and the resulting effect on the refractive index were evaluated using UV/vis is spectroscopy and gas adsorption. Results from spectroscopy reflected the total

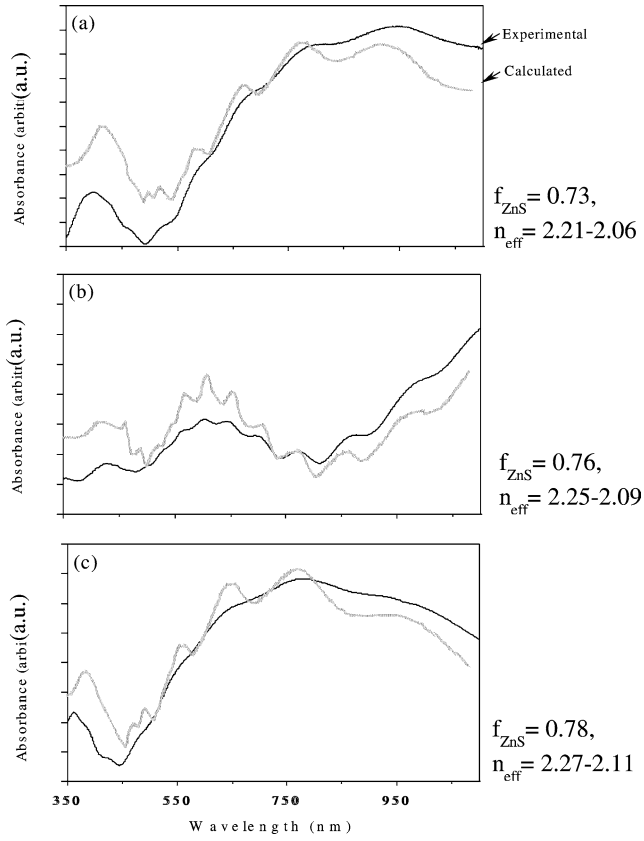

Fig. 3. Extinction spectra calculated using Mie theory superimposed on experimental spectra.

porosity (open and closed pores), while nitrogen adsorption data provided the detailed pore size and size distribution of the open porosity accessible to the gas molecules. Such open porosity can be utilized for the infiltration of higher-refractive-index material such as SnS_2 ($n = 3.3$–3.7) in order to produce inorganic composite particles with high refractive index.

Fig. 3 shows experimental UV/vis absorption spectra for aqueous colloidal suspensions of ZnS particles fit to curves derived from Mie scattering theory simulations. The spectra showed numerous resonance features that reflect the change in the scattering efficiency of the particles as a function of wavelength [13]; i.e., spectra exhibited short-range oscillations superimposed on a long-range wave structure that extended over the entire spectral range. The experimental observation of short-range Mie resonance features is only possible when spheres are sufficiently monodisperse [14]. A low degree of polydispersity in the particle system is important for obtaining highly ordered photonic crystal structures.

For the simulations, particle sizes were fixed to the average values determined by SEM image analysis and only the zinc sulfide fraction was varied. The filling fractions that resulted in the best fit of the long-range wave structures above the absorption edge of ZnS were 0.73, 0.76, and 0.78 for Figs. 3a–3c, respectively. The average filling fraction of ZnS

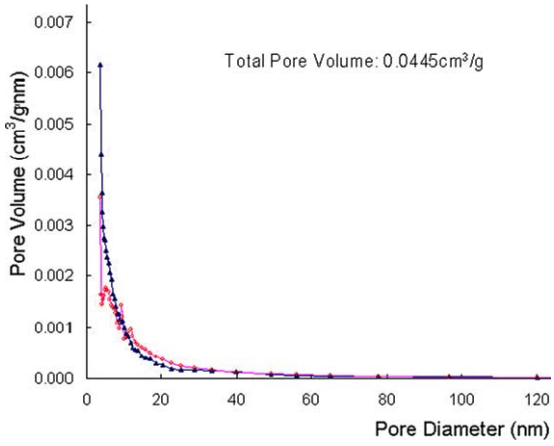

(a)

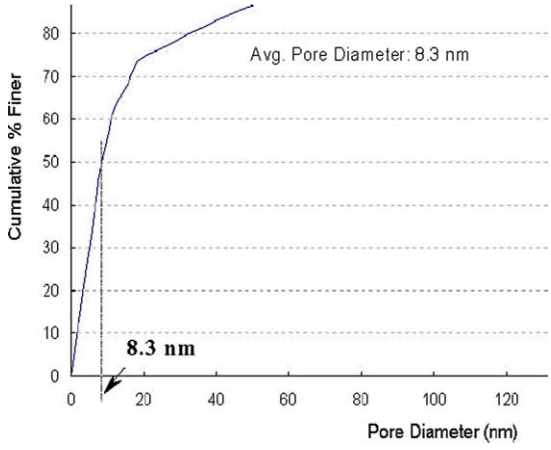

(b)

Fig. 4. (a) BJH pore volume vs pore diameter and (b) pore size distribution.

for samples with sphere sizes from 630 nm to 1.32 µm, was used to determine the average particle porosity as follows:

$$\text{porosity}_{\text{Mie}} = (1 - f_{\text{ZnS}}) \times 100\% = (1 - 0.76) \times 100\% = 24\%.$$

The average effective refractive index of the particles in suspension ranged from 2.25 at 413 nm to 2.09 at 709 nm as determined from the relation

$$n_{\text{eff}} = f_{\text{ZnS}} n_{\text{ZnS}} + (1 - f_{\text{ZnS}}) n_{\text{water}}.$$

A total pore volume of 0.0445 cm^3/g was calculated at a relative pressure of 0.9907 on the desorption isotherm. The area under the desorption curve in Fig. 4a, BJH pore volume vs diameter, represents the total pore volume. The open porosity was calculated from the BJH total pore volume as follows:

$$\text{porosity}_{\text{BJH}} = \frac{\text{total pore volume}}{\text{solid volume} + \text{total pore volume}} \times 100\% = \frac{0.0445\ \text{cm}^3/\text{g}}{1/(4.1\ \text{g/cm}^3) + 0.0445\ \text{cm}^3/\text{g}} \times 100\% = 15\%.$$

The porosity determination of 15% by gas adsorption differed from that estimated using optical methods (24%). This indicated that ∼9% of the pores were closed pores or voids. An average pore size of 8.3 nm was determined from the pore size distribution in Fig. 4b at a cumulative percentage finer than value of 50%. Though the presence of porosity in the particles lowered the refractive index below the bulk value, the ZnS colloids are still considered high-refractive-index building blocks relative to common colloidal materials such as silica and polystyrene ($n \sim 1.5$).

4. Summary

Uniform zinc sulfide colloidal clusters have been prepared and demonstrated as building blocks having morphology and optical properties suitable for photonic crystals. The precipitation method led to particles with high sphalerite phase purity and a stoichiometric composition of zinc and sulfur. Although the particles were found to be mesoporous as expected from the nanocrystalline aggregate internal structure, they still exhibited high refractive index. The colloids expand the menu of nonspherical particles that can be used for photonic crystal bases. Since there are few methods available to synthesize small nonspherical colloids of well-defined size and shape and high refractive index, the work is a fundamental step toward the realization of novel reduced-symmetry assemblies.

Acknowledgments

The authors acknowledge the support of the US Army Research Office MURI program under Contract DAAD19-01-1-0603. C.M. Liddell also thanks the Office of Naval Research for graduate fellowship support.

References

[1] V. Berger, Opt. Mater. 11 (1999) 131–142.
[2] J.D. Joannopoulos, P.R. Villeneuve, S. Fan, Nature 386 (1997) 143–149.
[3] T.F. Krauss, R.M. De la Rue, Prog. Quant. Electron. 23 (1999) 51–96.
[4] D.J. Norris, Y.A. Vlasov, Adv. Mater. 13 (2001) 371–376.
[5] Z.Y. Li, Z.Q. Zhang, Adv. Mater. 13 (2001) 433–436.
[6] Z. Li, J. Wang, B. Gu, J. Phys. Soc. Jpn. 67 (1998) 3288–3291.
[7] E. Yablonovitch, K.M. Leung, Physica B 175 (1991) 81–86.
[8] C. Murray, MRS Bull. 23 (1998) 33–38.
[9] D.M. Wilhelmy, E. Matijevic, J. Chem. Soc. Faraday Trans. 80 (1984) 563–570.
[10] R. Vacassy, S.M. Scholz, J. Dutta, C.J.G. Plummer, B. Houriet, H. Hofmann, J. Am. Ceram. Soc. 81 (1998) 2699–2705.
[11] G. Subramania, K. Constant, R. Biswas, M.M. Siglas, K.M. Ho, J. Lightwave Technol. 17 (1999) 1970–1974.
[12] M.L. Breen, A.D. Dinsmore, R.H. Pink, S.B. Qadri, B.R. Ratna, Langmuir 17 (2001) 903–907.
[13] S.M. Scholz, R. Vacassy, J. Dutta, H. Hofmann, M. Akinc, J. Appl. Phys. 83 (1998) 7860–7866.
[14] S.M. Scholz, R. Vacassy, L. Lemaire, J. Dutta, H. Hofmann, Appl. Organomet. Chem. 12 (1998) 327–335.